

Hydrogenated amorphous silicon oxide ($a\text{-SiO}_x\text{:H}$) single junction solar cell with 8.8% initial efficiency by reducing parasitic absorptions

Kim, Do Yun; Guijt, Erwin; van Swaaij, René A.C.M.M.; Zeman, Miro

DOI

[10.1063/1.4979690](https://doi.org/10.1063/1.4979690)

Publication date

2017

Document Version

Final published version

Published in

Journal of Applied Physics

Citation (APA)

Kim, D. Y., Guijt, E., van Swaaij, R. A. C. M. M., & Zeman, M. (2017). Hydrogenated amorphous silicon oxide ($a\text{-SiO}_x\text{:H}$) single junction solar cell with 8.8% initial efficiency by reducing parasitic absorptions. *Journal of Applied Physics*, 121, 133103-1 - 133103-6. <https://doi.org/10.1063/1.4979690>

Important note

To cite this publication, please use the final published version (if applicable). Please check the document version above.

Copyright

Other than for strictly personal use, it is not permitted to download, forward or distribute the text or part of it, without the consent of the author(s) and/or copyright holder(s), unless the work is under an open content license such as Creative Commons.

Takedown policy

Please contact us and provide details if you believe this document breaches copyrights. We will remove access to the work immediately and investigate your claim.

Hydrogenated amorphous silicon oxide ($a\text{-SiO}_x\text{:H}$) single junction solar cell with 8.8% initial efficiency by reducing parasitic absorptions

Cite as: J. Appl. Phys. **121**, 133103 (2017); <https://doi.org/10.1063/1.4979690>

Submitted: 18 December 2016 . Accepted: 23 March 2017 . Published Online: 05 April 2017

Do Yun Kim, Erwin Guijt, René A. C. M. M. van Swaaij, and Miro Zeman

COLLECTIONS

 This paper was selected as Featured



View Online



Export Citation



CrossMark

ARTICLES YOU MAY BE INTERESTED IN

[Amorphous silicon oxide window layers for high-efficiency silicon heterojunction solar cells](#)

Journal of Applied Physics **115**, 024502 (2014); <https://doi.org/10.1063/1.4861404>

[Optimized amorphous silicon oxide buffer layers for silicon heterojunction solar cells with microcrystalline silicon oxide contact layers](#)

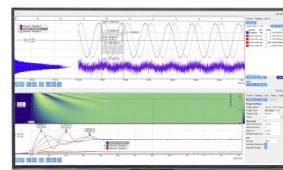
Journal of Applied Physics **113**, 134501 (2013); <https://doi.org/10.1063/1.4798603>

[Hydrogenated amorphous silicon oxide containing a microcrystalline silicon phase and usage as an intermediate reflector in thin-film silicon solar cells](#)

Journal of Applied Physics **109**, 113109 (2011); <https://doi.org/10.1063/1.3592208>

Challenge us.

What are your needs for periodic signal detection?



Zurich
Instruments

Hydrogenated amorphous silicon oxide (a-SiO_x:H) single junction solar cell with 8.8% initial efficiency by reducing parasitic absorptions

Do Yun Kim,^{a)} Erwin Guijt, René A. C. M. M. van Swaaij, and Miro Zeman

Laboratory of Photovoltaic Materials and Devices, Delft University of Technology, 2628 CD Delft, the Netherlands

(Received 18 December 2016; accepted 23 March 2017; published online 5 April 2017)

Hydrogenated amorphous silicon oxide (a-SiO_x:H) solar cells have been successfully implemented to multi-junction thin film silicon solar cells. The efficiency of these solar cells, however, has still been below that of state-of-the-art solar cells mainly due to the low J_{sc} of the a-SiO_x:H solar cells and the unbalanced current matching between sub-cells. In this study, we carry out optical simulations to find the main optical losses for the a-SiO_x:H solar cell, which so far was mainly optimized for V_{oc} and fill-factor (FF). It is observed that a large portion of the incident light is absorbed parasitically by the p-a-SiO_x:H and n-a-SiO_x:H layers, although the use of these layers leads to the highest $V_{oc} \times FF$ product. When a more transparent and conductive p-nc-SiO_x:H layer is substituted for the p-a-SiO_x:H layer, the parasitic absorption loss at short wavelengths is notably reduced, leading to higher J_{sc} . However, this gain in J_{sc} by the use of the p-nc-SiO_x:H compromises the V_{oc} . When replacing the n-a-SiO_x:H layer for an n-nc-SiO_x:H layer that has low n and k values, the plasmonic absorption loss at the n-nc-SiO_x:H/Ag interfaces and the parasitic absorption in the n-nc-SiO_x:H are substantially reduced. Implementation of this n-nc-SiO_x:H leads to an increase of the J_{sc} without a drop of the V_{oc} and FF. When implementing a thinner p-a-SiO_x:H layer, a thicker i-a-SiO_x:H layer, and an n-nc-SiO_x:H layer, a-SiO_x:H solar cells with not only high J_{sc} but also high V_{oc} and FF can be fabricated. As a result, an 8.8% a-SiO_x:H single junction solar cell is successfully fabricated with a V_{oc} of 1.02 V, a FF of 0.70, and a J_{sc} of 12.3 mA/cm², which is the highest efficiency ever reported for this type of solar cell. *Published by AIP Publishing.*

[<http://dx.doi.org/10.1063/1.4979690>]

I. INTRODUCTION

Hydrogenated amorphous silicon oxide (a-SiO_x:H) has a higher energy band gap (E_g) than typical hydrogenated amorphous silicon (a-Si:H), and therefore, a-SiO_x:H solar cells can convert high energy photons more efficiently into electricity with reduced thermalization loss. Consequently, a-SiO_x:H single-junction solar cells (SJSCs) can show a relatively higher open-circuit voltage and fill-factor product ($V_{oc} \times FF$) than typical a-Si:H SJSCs, provided the defect density induced by oxygen incorporation remains sufficiently low. Various studies have shown the successful development of decent quality intrinsic and doped a-SiO_x:H layers and subsequently these *optimized* a-SiO_x:H layers have been extensively applied to SJSCs, double-junction solar cells (DJSCs), triple-junction solar cells (TJSCs), and quadruple-junction solar cells (QJSCs) in the past few years.^{1–5} These a-SiO_x:H solar cells have shown outstanding solar-cell performance in terms of $V_{oc} \times FF$ and their light-induced degradation was comparable to that of typical a-Si:H solar cells. From theoretical calculations, it was concluded that the E_g of the *optimized* a-SiO_x:H absorber layers is close to the ideal E_g needed for the top-cell of TJSCs if the E_g of a bottom-cell is fixed at 1.1 eV, which roughly corresponds to the E_g of hydrogenated nano-crystalline silicon (nc-Si:H).^{4,6} In this

case, the TJSC can reach its maximum efficiency with the top-cell E_g of 2.0~2.3 eV and the middle-cell E_g of 1.40~1.50 eV. The former corresponds to the E_g of a-SiO_x:H and the latter corresponds to the E_g of hydrogenated amorphous silicon germanium (a-SiGe:H). Yan *et al.* reported the world record initial efficiency of 16.3% for Si-based thin film TJSCs with the structure of a-Si:H/a-SiGe:H/nc-Si:H.⁷ Considering the optimum band gap combination, the efficiency can be, in principle, increased further by the use of an a-SiO_x:H top-cell instead of an a-Si:H top sub-cell. In addition, such a high V_{oc} a-SiO_x:H solar cell can be a very interesting option when implemented in 4-terminal tandem solar cells.⁸ However, the improvement can be achievable only when the a-SiO_x:H top-cell generates enough photocurrent and, for a multijunction solar cell, current matching between all sub-cells is realized in the final device. In our previous work,⁴ we observed that the performance of *optimized* a-SiO_x:H solar cells deteriorated considerably when the absorber layer thickness increases, while the influence of the absorber layer thickness on typical a-Si:H solar-cell performance is not as strong.⁹ It was observed that the J_{sc} of a-SiO_x:H solar cells first increased as the thickness of a-SiO_x:H absorber layers increased but rapidly dropped when the thickness increases beyond a certain critical value. The $V_{oc} \times FF$ product of a-SiO_x:H solar cells also tended to drop continuously with increasing absorber-layer thickness resulting in low efficiency. For this reason, the thickness of a-SiO_x:H solar cells could be varied only in a limited range (up to

^{a)} Author to whom correspondence should be addressed. Electronic mail: d.kim@fz-jeulich.de. Present address: Institute of Photovoltaics, Forschungszentrum Jülich GmbH, Jülich 52425, Germany

200~250 nm), which limited the possibility to increase the photocurrent of a-SiO_x:H solar cells. In addition, it is also well-known that light degradation becomes more significant with thicker absorbers.^{9,10} In order to increase the J_{sc} of a-SiO_x:H solar cells further while maintaining the $V_{oc} \times FF$ product as high as possible with the limited absorber thickness, it is necessary to make the best use of the incident sunlight with the least photon loss. Therefore, in this contribution, we show how we have reduced parasitic absorption in the solar cell in order to obtain higher J_{sc} while maintaining the $V_{oc} \times FF$ product. For this purpose, different amorphous and nanocrystalline p- and n-type SiO_x:H layers having distinct optical constants and electrical properties are compared and employed in solar cells. We also carried out optical simulations of a-SiO_x:H solar cells to find out which photons do not contribute to the J_{sc} of solar cells but are lost for energy conversion through reflection and parasitic absorption. In this way, the full potential of *optimized* a-SiO_x:H solar cells is evaluated and breakthroughs for higher J_{sc} are presented and discussed. The electrical properties of devices are simultaneously evaluated as well so that the optical gain does not compromise the electrical performance of a-SiO_x:H single-junction solar cells.

II. EXPERIMENTAL DETAILS

In this study, the a-SiO_x:H single junction solar cells were fabricated with the following p-i-n structure: Asahi VU (SnO₂:F)/10 nm ZnO:Al/p-SiO_x:H/i-a-SiO_x:H (buffer)/i-a-SiO_x:H (absorber)/n-SiO_x:H/metal; the back metal contact consists of a stack of 150 nm Ag, 30 nm Cr, and 300 nm Al. On top of the SnO₂:F (the top transparent conductive oxide (TCO)), a 10-nm thick ZnO:Al layer was deposited, because the intense H₂-rich plasma can lead to the formation of oxygen-depleted surface regions (Sn precipitation) in the SnO₂:F layer during p-type layer deposition,¹¹ which can degrade the solar cell performance. All SiO_x:H layers were fabricated by radio frequency (RF, 13.65 MHz) plasma-enhanced chemical vapor deposition (PECVD). The detailed deposition conditions of doped and intrinsic a- and nc-SiO_x:H layers used to fabricate solar cells in this study are tabulated in Table I.

All solar cells were fabricated with the same buffer (*B*) and absorber (*I*) layers, but with different doped layers among *P1*, *P2*, *N1*, and *N2*. The combination of doped layers used for solar cells will be clearly stated throughout this

manuscript. Note that for *P2* a very high P_{RF} of 245 mW/cm² was used to achieve high crystallinity. The i-a-SiO_x:H absorber (*I*) used in this study contains an oxygen concentration of 3~5 at.% and has an optical band gap at an absorption of 10⁴ cm⁻¹ (E_{04}) of 2.1 eV.³ So far, this *I* has been employed successfully in various single- and multi-junction thin film silicon solar cells as an absorber layer and showed very high V_{oc} s and FFs.³⁻⁵ The photo J - V curves of solar cells were measured at standard 1-sun illumination (AM 1.5; 100 mW/cm²). For solar-cell characterization, the performance of 10 devices with an area of 0.16 cm² was measured using a Pasan IId Flash Solar Simulator and averaged. The maximal standard deviation in the measured parameters is 2 mV for the V_{oc} ; 0.04 mA/cm² for the short-circuit current density, J_{sc} ; 0.01 for the FF; and 0.05% for the energy conversion efficiency. The external quantum efficiency (EQE) was measured using an in-house built setup from which J_{sc} of solar cells is obtained. To investigate the optical properties of devices, optical simulations were performed using the optical model *GenPro4* implemented in the ASA simulator, which has been developed at Delft University of Technology,^{5,12-14} The *GenPro4* model is capable of dealing with both incoherent and coherent light for calculating transmittance, reflectance, and absorbance of the medium. In addition, the scalar scattering theory and ray tracing can be handled in this model, which describes light scattering behavior at rough interfaces. In our simulations, we used the scalar scattering theory to evaluate light scattering properties, which has been shown to be accurate for textured substrates with a relatively small rms roughness of up to ~220 nm.¹⁵⁻¹⁸ Thus, the scalar scattering theory describes well the light scattering at surfaces of the Asahi VU substrate and typical ZnO substrates used for thin film silicon solar cells. The actually fabricated materials are deployed in this optical simulation and their refractive index (n) and extinction coefficient (k), as obtained from photothermal deflection spectroscopy (PDS) and Fourier transform photocurrent spectroscopy (FTPS), are used as input parameters. In particular, nc-SiO_x:H films were treated as if it is a single-phase material instead of considering each respective phase when their optical and electrical properties were measured. All individual films were characterized on layers with a thickness of around 100 nm. Atomic force microscopy (AFM) scans of 256 × 256 points over an area of 10 μm × 10 μm on the Asahi VU substrate were taken to obtain the height

TABLE I. Deposition conditions of various p, i, and n layers used to fabricate a-SiO_x:H solar cells in this study.

ID	Layer type	SiH ₄ (sccm)	H ₂ (sccm)	CO ₂ (sccm)	2% B ₂ H ₆ (sccm)	2% PH ₃ (sccm)	P_{RF}^a (mW/cm ²)	p_d^b (mbar)	T_h^c (°C)
<i>P1</i>	p-a-SiO _x :H	20.0	20	45.0	2.0	...	14	0.7	300
<i>P2</i>	p-nc-SiO _x :H	1.0	170	1.4	0.2	...	245	2.2	300
<i>B</i>	i-a-SiO _x :H	2.5	200	2.5	21	2.0	200
<i>I</i>	i-a-SiO _x :H	8.0	200	2.0	63	2.6	200
<i>N1</i>	n-a-SiO _x :H	40.0	40	2.0	...	11.0	28	0.6	300
<i>N2</i>	n-nc-SiO _x :H	1.0	100	1.6	...	1.2	70	1.5	300

^aRF power density.

^bDeposition pressure.

^cHeater temperature.

distribution functions, which are used as an input parameter for the scalar scattering model as described by Jäger *et al.*^{15–17}

III. RESULTS AND DISCUSSION

The V_{oc} of a-SiO_x:H solar cells is not only sensitive to the E_g and defect density of i-a-SiO_x:H absorbers but also to the E_g and activation energy (E_a) of p- and n-type layers.^{3,19} The higher the E_g and the lower the E_a of doped layers, the larger the built-in voltage across a solar cell. This built-in voltage determines the upper limit of the V_{oc} . In our previous study, we observed that the V_{oc} of a-SiO_x:H solar cells was maximized when the E_a of p- and n-doped layers was minimized. Consequently, with $P1$ and $N1$ the a-SiO_x:H solar cell showed the highest $V_{oc} \times FF$ product. In Table II, the optical and electrical properties of $P1$ and $N1$ are listed together with $P2$ and $N2$. $P2$ and $N2$ were used to both a-Si:H and nc-Si:H sub-cells in multi-junction solar cells, forming excellent tunneling junctions because of their high electrical conductivities (σ_d) and low E_a .⁴ The crystalline fraction (X_c) of $P2$ and $N2$ as obtained from Raman spectroscopy is 37% and 62%, respectively, and as a result, their dark conductivities are substantially higher than those of the doped a-SiO_x:H layers ($P1$ and $N1$).

In Figs. 1(a) and 1(b), n and k of the doped layers are presented as a function of wavelength. From this figure, it is confirmed that both $P2$ and $N2$ have much lower n and k values than $P1$ and $N1$ over the entire measurement wavelength range, respectively.

In particular, the refractive index (n) of $N2$ is much smaller than that of I ; at a wavelength of 600 nm, n is 2.2 for $N2$ and 4.1 for I . This big difference in refractive index can lead to higher reflection at the i/n interface and thus higher absorption in an absorber. Čampa *et al.* demonstrated with experiments and simulations that the photocurrent of a-Si:H top cells in tandem cells can be higher due to more reflection when the refractive index of n-nc-SiO_x:H intermediate reflector layers is lower.²⁰ In addition, the use of n-nc-SiO_x:H with a low refractive index suppresses plasmonic absorption loss at the n-layer/Ag interface of the solar cells, enabling higher J_{sc} . Fig. 2(b) shows that the imaginary part of the refractive index (k) of $P2$ and $N2$ is much lower than that of $P1$ and $N1$, respectively, leading to higher E_{04} as indicated by the dotted orange line and in Table II. Note that the k of $N1$ is even higher than that of the i-a-SiO_x:H absorber layer. Thus, $P2$ and $N2$ have a potential to reduce the parasitic absorption and improve electrical transport at the same time. Due to these promising optical and electrical properties, p-nc-SiO_x:H and n-nc-SiO_x:H layers have been widely

TABLE II. The activation energy E_a , dark conductivity σ_d , crystalline fraction X_c , and optical band gap E_{04} of the doped layers.

ID	Layer type	E_a (eV)	σ_d (S/cm)	X_c (%)	E_{04} (eV)
$P1$	p-a-SiO _x :H	0.43	7×10^{-7}	...	2.17
$P2$	p-nc-SiO _x :H	0.15	2×10^{-3}	37	2.30
$N1$	n-a-SiO _x :H	0.21	1×10^{-2}	...	1.94
$N2$	n-nc-SiO _x :H	0.10	2.6	62	2.65

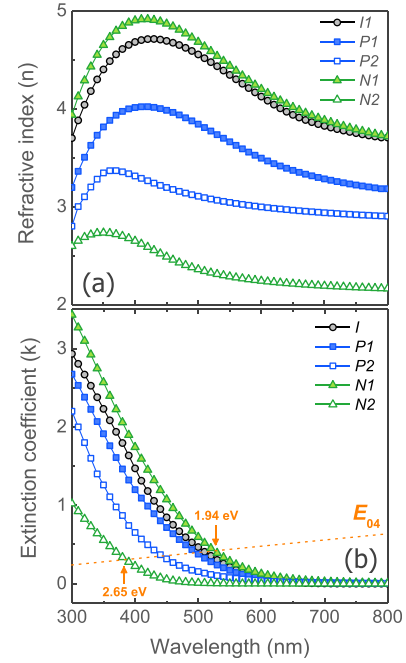


FIG. 1. (a) The real part of the refractive index (n) and (b) the extinction coefficient (k) as a function of wavelength of various silicon thin films used to fabricate solar cells in this study. From the wavelength dependence of k , the band gap E_{04} of the material was obtained. The guide line for E_{04} is indicated by the orange dotted line in (b).

implemented to a-Si:H and nc-Si:H solar cells by several groups.^{21–30}

To evaluate the effect of these doped layers on a-SiO_x:H solar cells, several solar cells with $P1$, $P2$, $N1$, and $N2$ are

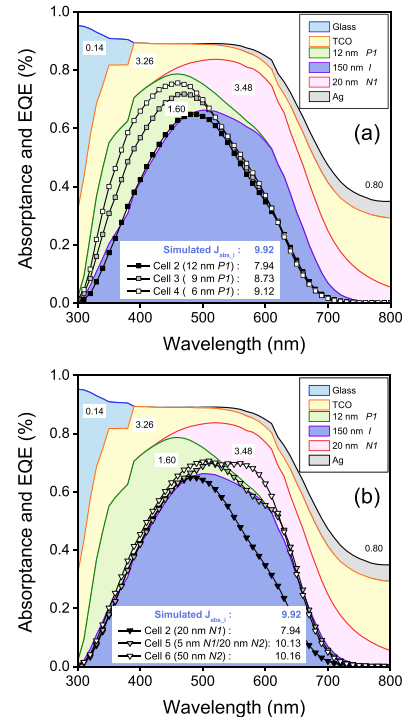


FIG. 2. EQEs of a-SiO_x:H solar cells with (a) different $P1$ thickness and (b) different n-layer configurations. Simulated absorbances (A_{sim}) of 12-nm thick $P1$ + 150-nm thick I and 150-nm thick I + 20-nm thick $N1$ are also included with colored areas. The current density values in the figures are given in mA/cm².

fabricated and their optical and electrical performances are discussed together with optical simulations. First of all, an a-SiO_x:H solar cell was fabricated with more transparent *P2* (30 nm) as a substitution for *P1* to reduce parasitic absorption. This solar cell will be called Cell 1 and a solar cell with 12 nm *P1* will be referred to as Cell 2. In Table III, their PV parameters are listed.

As remarked above, the *k* of *P2* is substantially lower than of *P1*. As a result, the J_{sc} of the a-SiO_x:H solar cell increased from 7.94 mA/cm² to 9.1 mA/cm² because of reduced parasitic absorption. However, it was observed that the increase in the J_{sc} compromised the V_{oc} . Even though *P2* had a much lower E_a (0.15 eV) than *P1* (0.43 eV), the built-in voltage that determines the upper limit of V_{oc} decreased by the use of *P2* because *P2* is based on nanocrystalline silicon material and has a lower mobility band gap than the amorphous-silicon based material used for *P1*. Consequently, the V_{oc} of the solar cell with *P2* ended up at only 0.87 V. This combination between V_{oc} decrease and J_{sc} increase reduced the efficiency slightly from 6.0% to 5.8%.

Therefore, instead of using *P2*, the thickness of *P1* is decreased from 12 nm to 6 nm in an attempt to reduce the parasitic absorption of Cell 2 without affecting the V_{oc} . The effect on the EQE of these cells (Cells 3 and 4) is shown in Fig. 2(a). In this figure, the simulated absorptance (A_{sim}) for Cell 2, whose $V_{oc} \times FF$ product is the highest of all cells used in this study, and the measured EQE of Cell 2, Cell 3, and Cell 4 are depicted together. There are two important observations to be noted in this figure. First, a significant mismatch between the A_{sim} of *I* (violet colored region) and the measured EQE of Cell 2 (black markers) is observed in the wavelength range of 500–750 nm. This difference is about 2.0 mA/cm². Second, substantial parasitic absorption in the TCO and doped layers results in an even higher photocurrent density loss of more than 9 mA/cm². We will now discuss these observations in somewhat more detail.

Ideally, the A_{sim} of *i*-layers and the EQE of solar cells are identical because only the photo-generated carriers in the *i*-layers can fully contribute to the J_{sc} of the solar cells unless recombination limits carrier collection. However, absorption at the *NI/Ag* interface of the solar cells is larger due to the plasmonic absorption of the nanorough Ag,³¹ reducing the actual absorption in *I* at long wavelengths. This plasmonic absorption has not been taken into account in the optical simulation shown in Figs. 2(a) and 2(b). This observation is in line with the results found in the literature³¹ in which Demontis *et al.* theoretically and experimentally investigated a-Si:H solar cells with various metal contacts and dielectric

materials inserted between the metal contacts and the n-a-Si:H. They found that plasmonic absorption at the n-a-Si:H/metal interfaces is largely dependent on the optical constants of metals and the inserted dielectric materials. When the dielectric layer has a larger refractive index, *n*, localized plasmon resonance occurs at longer wavelengths, leading to plasmonic absorption.^{32,33} Simulation results clearly show that a large portion of the incident light is absorbed in the TCO and doped layers besides the *i*-layer and this parasitically absorbed light does not contribute to J_{sc} . The total parasitic absorption in the glass, TCO, 12-nm thick p-a-SiO_x:H, 20-nm thick n-a-Si_xO:H, and Ag sums up to an equivalent current density of 9.28 mA/cm², which is even higher than the J_{sc} of Cell 2. In particular, the parasitic absorption in the doped layers (*P1* and *NI*) accounts for more than half the total parasitic absorption. From these simulations, it is obvious that there is significant room to increase the J_{sc} of the a-SiO_x:H solar cell by reducing the parasitic absorption without varying the absorber layer thickness.

As the thickness of *P1* decreases from 12 nm to 6 nm, the EQE of the solar cell increases for short wavelengths because less incident light is absorbed by the thinner *P1* layer. As a result, the J_{sc} increases from 7.94 mA/cm² to 9.12 mA/cm². In this case, the parasitic absorption loss of 6 nm *P1* is only 0.47 mA/cm² as concluded from simulations. The V_{oc} and FF were found to decrease slightly from 1.02 V to 0.98 V and from 0.74 to 0.71, respectively, as the *P1* thickness decreases from 12 nm to 6 nm, probably due to the reduced internal electric field with the thinner *p*-layer as a substantial part of this layer will be depleted. The light *J-V* curves of Cell 1, Cell 2, Cell 3, and Cell 4 are shown in Fig. 3. Although the V_{oc} and FF decrease, the efficiency increases from 6.0% to 6.4% thanks to the J_{sc} increase. It is interesting to recall that *P1* has a substantially lower electrical conductivity than *P2* by four orders of magnitude but still results in excellent PV performance with a series resistance of 8.37 Ω·cm² (Cell 2). This value is not much larger than when the more conductive 30 nm *P2* was used (6.72 Ω·cm²). It is likely that these devices are less influenced by the conductivity of doped layers because of the relatively small photocurrent density.

In Fig. 2(b), the EQEs of three different a-SiO_x:H solar cells are shown with 20-nm thick *NI* (Cell 2), 4-nm thick *NI*+50 nm *N2* (Cell 5), and 50-nm thick *N2* (Cell 6). As mentioned above, the difference between the A_{sim} of *I* and the measured EQE of the solar cells is due to plasmonic absorption at the *NI*-Ag interface, which has not been taken into account in this simulation. The plasmonic absorption

TABLE III. PV parameters of a-SiO_x:H solar cells with different doped layers. The thickness of *I* is kept constant at 150 nm.

ID	<i>P1</i> thickness (nm)	<i>P2</i> thickness (nm)	<i>NI</i> thickness (nm)	<i>N2</i> thickness (nm)	V_{oc} (mV)	J_{sc} (mA/cm ²)	<i>FF</i> (-)	Eff.(%)
Cell 1		30	20	...	0.87	9.10	0.74	5.8
Cell 2	12		20	...	1.02	7.94	0.74	6.0
Cell 3	9		20	...	1.01	8.73	0.72	6.3
Cell 4	6		20	...	0.98	9.12	0.71	6.4
Cell 5	12		4	50	1.02	10.13	0.73	7.5
Cell 6	12		...	50	1.01	10.61	0.73	7.8

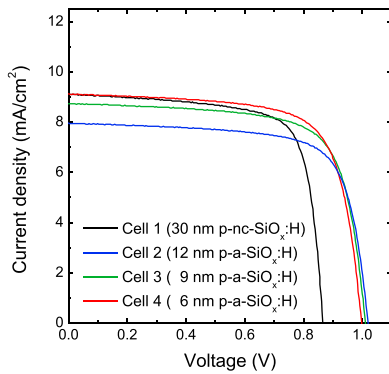


FIG. 3. Photo J - V curves of Cell 1, Cell 2, Cell 3, and Cell 4 with different p-layers.

losses are reduced by the use of $N2$ because this material has much lower n (2.2 at 600 nm). When an interlayer having low n is embedded in between a silicon solar cell and a metal back contact, a shift of the localized plasmon resonances to shorter wavelengths is induced, and consequently, the plasmonic absorption pattern shows a strong blue shift. Moreover, $N2$ has very small k -values over the entire wavelength range (see Fig. 1(b)), and as a result, its absorption is much lower compared to $N1$. Consequently, the EQE of the a-SiO_x:H solar cells in the wavelength range of 480 nm to 800 nm increases substantially as the thickness of $N1$ is reduced (Cell 5) and finally completely replaced with $N2$ (Cell 6). The measured EQE of Cell 6 is larger than the A_{sim} of I because the photons, which were parasitically absorbed in $N1$ for Cell 2, are not absorbed in $N2$ but I for Cell 6. The J_{sc} increases from 7.94 mA/cm² for Cell 2 to 10.61 mA/cm² for Cell 6 that only has an $N2$ layer, while the V_{oc} and FF stay almost constant at 1.01 V and 0.73, respectively, resulting in an efficiency of 7.8%.

Finally, an a-SiO_x:H solar cell is fabricated with the combination of a 9-nm thick PI , 200-nm thick I , and 50-nm thick $N2$; hereafter called Cell 7. Note that not a 6-nm thick but a 9-nm thick PI was implemented to make sure that the internal electric field in the intrinsic layer is maintained and thus keeps the V_{oc} and FF sufficiently high. In addition, only a 200 nm thick I was used to enhance the J_{sc} because the $V_{oc} \times FF$ product of a-SiO_x:H solar cells was found to deteriorate considerably for absorber thicknesses beyond this value.⁴ Therefore, the thickness of PI and I and thereby J_{sc} and $V_{oc} \times FF$ were compromised to reach the maximal efficiency in this study. As a result, this solar cell showed a V_{oc} of 1.02 V, a FF of 0.70, a J_{sc} of 12.3 mA/cm², and an efficiency of 8.8%, which to our knowledge is the highest efficiency ever reported for a-SiO_x:H single junction solar cells. The EQE and photo J - V curve of Cell 7 are presented in Figs. 4(a) and 4(b), respectively. Also, the A_{sim} of Cell 7 with a 210 nm thick i-layer is shown in Fig. 4(a). In this case, the EQE and the A_{sim} of I match very well even at long wavelengths because $N2$ has a very low n , leading to the sufficient suppression of the plasmonic absorption at the $N2/Ag$ interface. A thinner PI and more transparent $N2$ decrease the parasitic absorption by 3.57 mA/cm² as compared to Cell 2. The thicker I contributes to the increase in J_{sc} without affecting the $V_{oc} \times FF$ product very much.

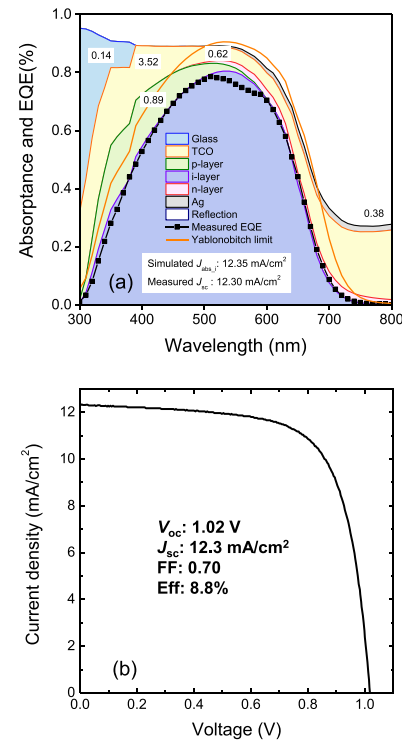


FIG. 4. (a) Simulated absorption spectra (colored areas) with a 210 nm thick i-layer and measured external quantum efficiency (black markers) of the a-SiO_x:H solar cell with a 200 nm thick i-layer (Cell 7) and (b) the photo J - V curve of Cell 7. The Yablonovitch limit^{34,35} (orange line) is also represented in (a), taking into account parasitic absorptions.

It should be noted that Cell 7 was fabricated on the Asahi VU substrate, whose root-mean-square roughness is only about 34 nm.³ Therefore, the full potential of this a-SiO_x:H cell is evaluated according to the theoretical absorption limit proposed by Yablonovitch.^{34,35} The results are presented in Fig. 4(a) with the orange line. For the calculations, the parasitic absorptions of glass, TCO, and doped layers were taken into account to scale down the incident light. Both theoretical calculations suggest that the J_{sc} can increase further by better light scattering as shown in Fig. 4(a); an equivalent current density of 15.43 mA/cm² by Yablonovitch limit. Therefore, there is still more room to increase the J_{sc} by implementing more transparent p- and TCOs layers and by using more textured TCOs.

IV. CONCLUSION

We carried out optical simulations for the a-SiO_x:H solar cell that had been optimized mainly for high V_{oc} and FF so far. From the simulations, it was observed that a large portion of the incident light was parasitically absorbed by p-a-SiO_x:H and n-a-SiO_x:H. Also, it was found that the plasmonic absorption at the n-a-SiO_x:H/Ag interface reduced the long wavelength response, resulting in a low J_{sc} . When more transparent and conductive p-nc-SiO_x:H is substituted for p-a-SiO_x:H, the parasitic absorption loss at short wavelengths was notably reduced, leading to higher J_{sc} . However, the gain in J_{sc} by the use of the p-nc-SiO_x:H compromised the V_{oc} , and thus, the efficiency of a-SiO_x:H solar cell decreased. On the other hand, when using n-nc-SiO_x:H with

low n and k values, the plasmonic absorption loss at the n-nc-SiO_x:H/Ag interface was largely removed and the parasitic absorption in the n-nc-SiO_x:H was substantially reduced. This result leads to a J_{sc} increase without losing V_{oc} and FF. Finally, a thinner p-a-SiO_x:H, a thicker i-a-SiO_x:H, and a more transparent n-nc-SiO_x:H are implemented to fabricate a high- J_{sc} and high- V_{oc} a-SiO_x:H solar cell. As a result, an 8.8% a-SiO_x:H single junction solar cell was fabricated successfully with a V_{oc} of 1.02 V, a FF of 0.70, and a J_{sc} of 12.3 mA/cm², which to our knowledge is the highest efficiency ever reported for this type of solar cell.

ACKNOWLEDGMENTS

This work was carried out in the framework of the FP7 project “Fast Track,” funded by the EC under Grant Agreement No. 283501. We are grateful to Dr. Rudi Santbergen for the valuable discussions. We would like to thank Martijn Tijssen, Stefaan Heirman, and Remko Koornneef from PVMD group of Delft University of Technology for the technical assistance with the deposition systems and measurement setups.

- ¹S. Inthisang, K. Sriprapha, S. Miyajima, A. Yamada, and M. Konagai, *Jpn. J. Appl. Phys., Part 1* **48**, 122402 (2009).
- ²S. Inthisang, T. Krajangsang, I. A. Yunaz, A. Yamada, M. Konagai, and C. R. Wronski, *Phys. Status Solidi C* **8**, 2990 (2011).
- ³D. Y. Kim, E. Guijt, R. A. C. M. M. van Swaaij, and M. Zeman, *Prog. Photovoltaics: Res. Appl.* **23**, 671 (2015).
- ⁴D. Y. Kim, E. Guijt, F. T. Si, R. Santbergen, O. Isabella, R. A. C. M. M. van Swaaij, and M. Zeman, *Sol. Energy Mater. Sol. Cells* **141**, 148 (2015).
- ⁵F. T. Si, D. Y. Kim, R. Santbergen, H. Tan, R. A. C. M. M. van Swaaij, A. H. M. Smets, O. Isabella, and M. Zeman, *Appl. Phys. Lett.* **105**, 063902 (2014).
- ⁶I. A. Yunaz, H. Nagashima, D. Hamashita, S. Miyajima, and M. Konagai, *Sol. Energy Mater. Sol. Cells* **95**, 107 (2011).
- ⁷B. Yan, G. Yue, L. Sivec, J. Yang, S. Guha, and C.-S. Jiang, *Appl. Phys. Lett.* **99**, 113512 (2011).
- ⁸D. Zhang, W. Soppe, and R. E. I. Schropp, *Energy Procedia* **77**, 500 (2015).
- ⁹M. Stuckelberger, A. Billet, Y. Riesen, M. Boccard, M. Despeisse, J.-W. Schüttauf, F.-J. Haug, and C. Ballif, *Prog. Photovoltaics: Res. Appl.* **24**, 446 (2016).
- ¹⁰P. J. McElheny, S. S. Nag, S. J. Fonash, C. R. Wronski, M. Bennett, and R. Arya, in *21st IEEE Photovoltaic Specialists Conference* (1990), p. 1459.

- ¹¹H. Schade, Z. E. Smith, J. H. Thomas, and A. Catalano, *Thin Solid Films* **117**, 149 (1984).
- ¹²O. Isabella, A. H. M. Smets, and M. Zeman, *Sol. Energy Mater. Sol. Cells* **129**, 82 (2014).
- ¹³M. Zeman and J. Krc, *J. Mater. Res.* **23**, 889 (2008).
- ¹⁴M. Zeman, O. Isabella, S. Solntsev, and K. Jäger, *Sol. Energy Mater. Sol. Cells* **119**, 94 (2013).
- ¹⁵K. Jäger and M. Zeman, *Appl. Phys. Lett.* **95**, 171108 (2009).
- ¹⁶K. Jäger, M. Fischer, R. A. C. M. M. van Swaaij, and M. Zeman, *J. Appl. Phys.* **111**, 083108 (2012).
- ¹⁷K. Jäger, D. N. P. Linssen, O. Isabella, and M. Zeman, *Proc. SPIE* **2014**, 91400M.
- ¹⁸D. Y. Kim, R. A. C. M. M. van Swaaij, and M. Zeman, *IEEE J. Photovoltaics* **4**, 22 (2014).
- ¹⁹S. Nonomura, H. Okamoto, and Y. Hamakawa, *Appl. Phys. A* **32**, 31 (1983).
- ²⁰A. Čampa, M. Meier, M. Boccard, L. V. Mercaldo, M. Ghosh, C. Zhang, T. Merdžanova, J. Krč, F. J. Haug, and M. Topič, *Sol. Energy Mater. Sol. Cells* **130**, 401 (2014).
- ²¹P. D. Veneri, L. V. M. Mercaldo, and I. Usatii, *Appl. Phys. Lett.* **97**, 023512 (2010).
- ²²P. Cuony, M. Marending, D. T. L. Alexander, M. Boccard, G. Bugnon, M. Despeisse, and C. Ballif, *Appl. Phys. Lett.* **97**, 213502 (2010).
- ²³M. Despeisse, C. Battaglia, M. Boccard, G. Bugnon, M. Charrière, P. Cuony, S. Hänni, L. Löfgren, F. Meillaud, G. Parascandolo, T. Söderström, and C. Ballif, *Phys. Status Solidi A* **208**, 1863 (2011).
- ²⁴V. Smirnov, A. Lambertz, B. Grootoink, R. Carius, and F. Finger, *J. Non-Cryst. Solids* **358**, 1954 (2012).
- ²⁵P. D. Veneri, L. V. M. Mercaldo, and I. Usatii, *Prog. Photovoltaics: Res. Appl.* **21**, 148 (2013).
- ²⁶M. Despeisse, G. Bugnon, A. Feltrin, M. Stueckelberger, P. Cuony, F. Meillaud, A. Billet, and C. Ballif, *Appl. Phys. Lett.* **96**, 073507 (2010).
- ²⁷L. V. Mercaldo, P. Delli Veneri, I. Usatii, E. M. Esposito, and G. Nicotra, *Sol. Energy Mater. Sol. Cells* **119**, 67 (2013).
- ²⁸A. Lambertz, F. Finger, R. E. I. Schropp, U. Rau, and V. Smirnov, *Prog. Photovoltaics: Res. Appl.* **23**, 939 (2015).
- ²⁹P. Cuony, D. T. L. Alexander, I. Perez-Wurfl, M. Despeisse, G. Bugnon, M. Boccard, T. Söderström, A. Hessler-Wyser, C. Hébert, and C. Ballif, *Adv. Mater.* **24**, 1182 (2012).
- ³⁰S. Kim, J.-W. Chung, H. Lee, J. Park, Y. Heo, and H.-M. Lee, *Sol. Energy Mater. Sol. Cells* **119**, 26 (2013).
- ³¹V. Demontis, C. Sanna, J. Melskens, R. Santbergen, A. H. M. Smets, A. Damiano, and M. Zeman, *J. Appl. Phys.* **113**, 064508 (2013).
- ³²F.-J. Haug, T. Söderström, O. Cubero, V. Terrazoni-Daudrix, and C. Ballif, *J. Appl. Phys.* **104**, 064509 (2008).
- ³³J. Springer, A. Poruba, L. Müllerova, M. Vanecek, O. Kluth, and B. Rech, *J. Appl. Phys.* **95**, 1427 (2004).
- ³⁴E. Yablonoitch, *J. Opt. Soc. Am.* **72**, 899 (1982).
- ³⁵T. Tiedje, E. Yablonoitch, G. D. Cody, and B. G. Brooks, *IEEE Trans. Electron Devices* **31**, 711 (1984).